

REPORT DOCUMENTATION PAGE

AFRL-SR-AR-TR-06-0164

The public reporting burden for this collection of information is estimated to average 1 hour per response, including gathering and maintaining the data needed, and completing and reviewing the collection of information. Send comments information, including suggestions for reducing the burden, to Department of Defense, Washington Headquarters Service, 1215 Jefferson Davis Highway, Suite 1204, Arlington, VA 22202-4302. Respondents should be aware that notwithstanding any penalty for failing to comply with a collection of information if it does not display a currently valid OMB control number.

PLEASE DO NOT RETURN YOUR FORM TO THE ABOVE ADDRESS.

1. REPORT DATE (DD-MM-YYYY) 21-04-2006		2. REPORT TYPE Final Report		3. DATES COVERED (From - To) May 2002 - November 2005	
4. TITLE AND SUBTITLE Modeling of MEMS-Based Hydrogen Peroxide Monopropellant Micro-Thrusters				5a. CONTRACT NUMBER	
				5b. GRANT NUMBER USAF 49620-02-1-0230	
				5c. PROGRAM ELEMENT NUMBER	
6. AUTHOR(S) Darren L. Hitt				5d. PROJECT NUMBER	
				5e. TASK NUMBER	
				5f. WORK UNIT NUMBER	
7. PERFORMING ORGANIZATION NAME(S) AND ADDRESS(ES) Department of Mechanical Engineering University of Vermont Burlington, Vermont 05405				8. PERFORMING ORGANIZATION REPORT NUMBER	
9. SPONSORING/MONITORING AGENCY NAME(S) AND ADDRESS(ES) Dr. Mitat Birkan Space Propulsion and Power Air Force Office of Scientific Research 4015 Wilson Blvd. Arlington, VA 22203-1954				10. SPONSOR/MONITOR'S ACRONYM(S)	
				11. SPONSOR/MONITOR'S REPORT NUMBER(S)	
12. DISTRIBUTION/AVAILABILITY STATEMENT Approved for public release, distribution unlimited					
13. SUPPLEMENTARY NOTES					
14. ABSTRACT This document describes the three-year effort to develop computational methodologies for the modeling of a hydrogen-peroxide-based monopropellant micro-thruster operation. Computational models have been developed in two primary areas: (1) the numerical simulation of supersonic viscous flow in linear micro-nozzles; and (2) numerical simulation of chemical decomposition in micro-scale catalytic beds. In the case of the former, results are provided which describe the determination of "optimal" nozzle angles which maximize thrust production as a function of the flow conditions. This optimal angle was found to be approximately 25-30 degrees. Additional results delineate the importance of heat transfer and 3-D geometric effects. In the case of the latter, a combination of approximate, semi-analytical and fully computational models for simulating catalyzed monopropellant decomposition in micro-channels have been used to obtain predictions of minimum catalyst bed length required for complete decomposition; predictions suggest MEMS-compatible catalyst bed lengths of approximately 1-2mm are necessary.					
15. SUBJECT TERMS micropropulsion, hydrogen-peroxide, micro-nozzle, chemical decomposition, nanosats					
16. SECURITY CLASSIFICATION OF:			17. LIMITATION OF ABSTRACT	18. NUMBER OF PAGES 9	19a. NAME OF RESPONSIBLE PERSON Darren L. Hitt
a. REPORT	b. ABSTRACT	c. THIS PAGE			19b. TELEPHONE NUMBER (Include area code) 802-656-1940

DISTRIBUTION STATEMENT A
Approved for Public Release
Distribution Unlimited

D.L. Hitt, Univ. of Vermont

1

**AFOSR Final Progress Report:
Modeling of MEMS-Based Hydrogen
Peroxide Monopropellant Micro-Thrusters**

D. L. HITT
Principal Investigator
Department of Mechanical Engineering
College of Engineering & Mathematical Sciences
University of Vermont
Burlington, Vermont 05405

Grant #: USAF 49620-02-1-0230
Program Officer: Mitat Birkan, AFOSR

(3 May 2006)

This document describes the three-year effort to develop computational methodologies for the modeling of a hydrogen- peroxide-based monopropellant micro-thruster operation. Computational models have been developed in two primary areas: (1) the numerical simulation of supersonic viscous flow in linear micro-nozzles; and (2) numerical simulation of chemical decomposition in micro-scale catalytic beds. In the case of the former, results are provided which describe the determination of 'optimal' nozzle angles which maximize thrust production as a function of the flow conditions. This optimal angle was found to be approximately 25-30 degrees. Additional results delineate the importance of heat transfer and 3-D geometric effects. In the case of the latter, a combination of approximate, semi-analytical and fully computational models for simulating catalyzed monopropellant decomposition in micro-channels have been used to obtain predictions of minimum catalyst bed length required for complete decomposition; predictions suggest catalyst bed lengths of approximately 1-2 mm are necessary which are compatible with MEMS-type configurations.

1. Overview

The motivation for this project was originally derived from the PI's involvement in the development of a prototype hydrogen-peroxide-based monopropellant micro-thruster by propulsion engineers at NASA Goddard Space Flight Center (GSFC). This MEMS-based micro-thruster concept was intended to offer a potential solution for satisfying the challenging propulsion requirements needed for orbital positioning maneuvers by next-generation miniaturized satellites ('nanosats'). A photograph of the original GSFC prototype is shown in Fig. 1. In the development and subsequent testing of the prototype, two areas for important, applied research clearly presented themselves: (1) investigation of viscous impacts on supersonic nozzle flow on the micro-scale; and (2) prediction of monopropellant decomposition in micro-catalyst chambers/configurations. A summary of the work performed along with key findings is presented in the following sections.

20060614013

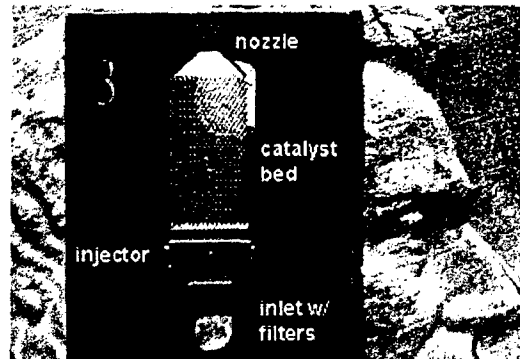


FIGURE 1. A photograph of the original NASA/GSFC hydrogen-peroxide micro-thruster prototype.

2. Numerical Simulations of Viscous Supersonic Flow in Linear Micro-Nozzles

2.1. Summary of Computational Efforts

The ongoing work involving the numerical simulation of supersonic flow in micro-nozzles has been targeted at investigating the specific impact(s) of viscous forces on the nozzle performance characteristics – notably the thrust production under varying flow and geometric conditions. Much of the work has focused on a systematic investigation of thrust production associated with decomposed monopropellants in 2-D linear micro-nozzles under varying flow conditions and for different nozzle angles. The motivation for this has been a search for an ‘optimal’ geometry is based on the notion that there is a trade-off between geometric losses realized at wider nozzle angles and viscous boundary layer ‘choking’ at smaller (traditional) nozzle angles. The restriction to a 2-D geometry is reasonably justified provided the extrusion depth of an actual 3-D MEMS thruster is significantly larger than the throat of the nozzle, which is indeed the case for the NASA/GSFC design. Nonetheless, some preliminary simulations of 3-D nozzles have also been performed as part of the overall effort. In terms of heat transfer modeling, while many of the simulations have assumed adiabatic walls for the nozzle, some additional effort has been placed in investigating the potential effects of heat transfer through the walls into the surrounding substrate. Lastly, instances of steady and transient flow have been examined. The former is a simplified but valuable tool for investigating the importance of viscous forces whereas the latter is a better representation of an actual nozzle operation.

2.2. The Computational Models

Continuum-based computational models for the supersonic micro-nozzle flow have been based on the design geometry and operating specifications of the NASA/GSFC microthruster nozzle. Flexibility was incorporated into the models to permit parametric studies of varying nozzle geometries, flow conditions, and monopropellant (hydrogen peroxide and hydrazine). The validity of a continuum model can be argued *a posteriori* by evaluating the Knudsen number of the flow within the region of interest and demonstrating that indeed rarefaction effects may be safely neglected if one is focused on the

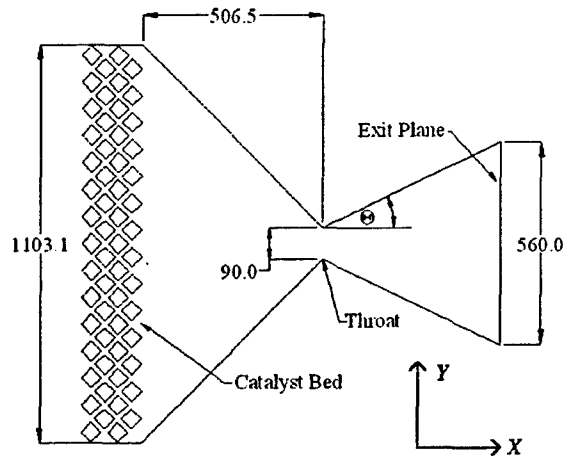


FIGURE 2. Geometry of NASA/GSFC prototype converging-diverging micro-nozzle for the monopropellant thruster. Note expander angle θ . All units are in microns. The depth of the device is varied.

thrust and impulse delivery.† Flexibility has been incorporated into the models to enable parametric studies for an arbitrary nozzle divergence angle θ while maintaining a fixed expansion ratio (see Fig. 2). The models include temperature-dependent thermophysical properties for the gases which permit simulation of decomposed monopropellant gases for cases of: (1) hydrogen peroxide; and (2) hydrazine. The latter was included in the work to provide a comparison for performance since the decomposed hydrazine will feature a notably lower gas viscosity and different temperature dependencies. Simulations have been performed for different mass flow rates (i.e., Reynolds numbers) for for primarily two ambient back-pressure conditions corresponding to instances of *under-expanded* and *pressure-matched* nozzle exit conditions.

All simulations have been performed using the FLUENT6 computational fluid dynamics software package on Linux CPU servers (Dell PowerEdge 2650, dual Xeon 2.8 GHz processors, 4 GB RAM) purchased under this grant.

2.3. Optimal Expansion Angle for 2-D Linear Micro-Nozzles

Here we provide summarizing plots which depict the key findings of the study. Complete details can be found in Louisos & Hitt (2005).‡

2.3.1. Micro-Nozzle Flow Characteristics for Varying θ , Re

Shown in Fig. 3 is a sample visualization of the Mach plumes for three different nozzle angles for a fixed mass flow rate ($Re = 650$); for these cases the flow is under-expanded. Simulations have also been performed for a fixed nozzle angle and for varying mass flow rates (see Fig. 4).

Clearly the nature of the plume depends on both geometry and exit pressure of the

† This of course would not be in the case if one were interested in the details of the exhaust plume where rarefaction effects require special treatment (e.g. Burnett equations, Monte Carlo gas dynamic simulations).

‡ Louisos W. and Hitt D.L., 2005, Optimal Expander Geometry for Viscous, Supersonic Flows in 2-D Micro-Nozzles, AIAA Paper 2005-5032

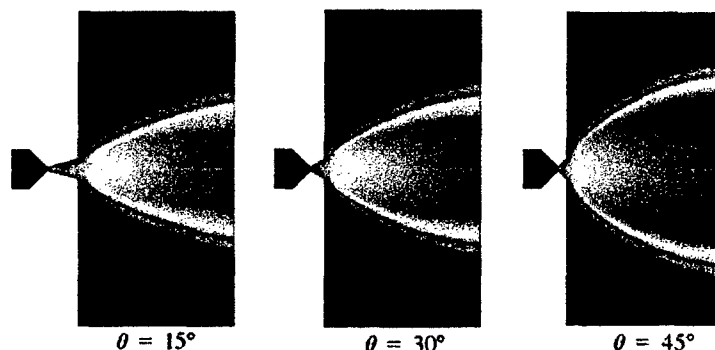


FIGURE 3. Plot of Mach contours for hydrogen peroxide, steady, 2-D, 15°, 30°, and 45° expander half-angle nozzle flow simulation exhausting to 1kPa ambient pressure. Note the expansion fan pattern as a result of the under-expanded supersonic flow at the nozzle exit

nozzle, with the later resulting in oblique shock or expansion fan phenomena depending on the mass flow rate. For each simulation, the extent of the subsonic region within the nozzle – a direct consequence of viscous effects – has been mapped out. The results for a fixed nozzle geometry as a function of Reynolds number are shown in Fig. 5. As the Reynolds number decreases, the size of the subsonic region increases and vice-versa; the presence of a larger subsonic region results in decreased thruster performance and efficiency and thus is clearly undesirable. Note that at sufficiently low Reynolds number ($Re \sim 20$ or less) even the centerline flow in the nozzle fails to remain supersonic upon reaching the exit plane. In all cases, the extent of the viscous subsonic layer is sufficient to substantially alter the exit flow from the nozzle.

2.3.2. Thrust Characteristics

From the numerical simulations the thrust production has been characterized as a function of nozzle geometry, mass flow rate and monopropellant. Shown in Fig. 6 is a plot of the thrust delivered as a function of the nozzle angle θ for hydrogen peroxide and hydrazine; the mass flow rate for these cases were held at the baseline design value set by NASA/GSFC for their prototype. For the case of hydrazine, it is seen that the thrust production is virtually insensitive to the nozzle angle for $\theta < 30^\circ$ after which point it diminishes owing to geometric losses associated with highly non-axial exit flow. In contrast, the performance of the hydrogen-peroxide flow reaches a peak production at a nozzle angle of $\theta \approx 30^\circ$ – a value roughly twice that which is typically found in macro-scale nozzles. This ‘optimal’ angle represents a trade-off between geometric losses and the ‘unclogging’ of the flow by widening the nozzle to compensate for viscous boundary layers. This optimization becomes even more pronounced in cases where the exiting nozzle flow is pressure-matched to the ambient conditions. The corresponding results for pressure-matched hydrogen peroxide flow is shown in Fig. 7 where the optimizing angle is seen to be approximately 28° .

2.3.3. Key Outcomes

In this study our objective was to obtain an understanding the interplay of nozzle geometry and viscous effects in supersonic micro-nozzles. To date we have successfully performed parametric simulations of hydrogen peroxide and hydrazine monopropellant

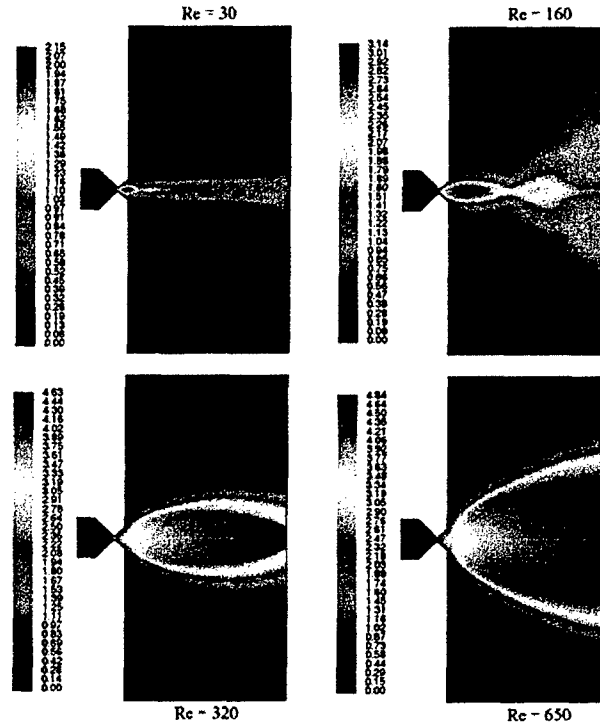


FIGURE 4. The Mach number contours for the 30° divergence half-angle hydrogen peroxide micro-nozzle for Reynolds numbers of 30, 160, 320, and 650 at the nozzle throat. At low Reynolds numbers, the flow is over-expanded and free boundary shock reflection occurs at the nozzle exit. However, as the Reynolds number is increased, the flow transitions from over-expanded to under-expanded and an expansion fan pattern develops at the nozzle exit, increasing the exhaust plume size and resulting in premature flow turning.

supersonic flow for expander half-angles in the range of $10\text{-}50^\circ$. It has been shown that viscous effects and the resulting subsonic boundary layer have a significant impact on micro-nozzle performance and efficiency. The existence of an optimal half-angle in the range of $25\text{-}30^\circ$ is a result of trade-offs between the size of the viscous boundary layer in the expander and losses in thrust due to non-axial flow components. The Reynolds number parametric analysis verifies the key role viscous effects play in determining the performance and efficiency of MEMS-based supersonic thruster nozzles. The viscous subsonic boundary layer has been quantified and is shown to occupy a large percentage of the flow field; approximately 15% at high mass flow rates and up to 100% at low Reynolds numbers. The value of the Reynolds number directly determines the thickness of the subsonic boundary layer. This is highlighted by the fact that as the Reynolds number becomes sufficiently large (i.e., $Re > 800$) the flow exhibits an inviscid nature, the subsonic boundary layer is diminished, and the performance curves collapse onto the quasi 1-D inviscid solution. The size of the subsonic region directly effects micro-nozzle performance and viscous effects represent a degradation in thruster performance and efficiency.

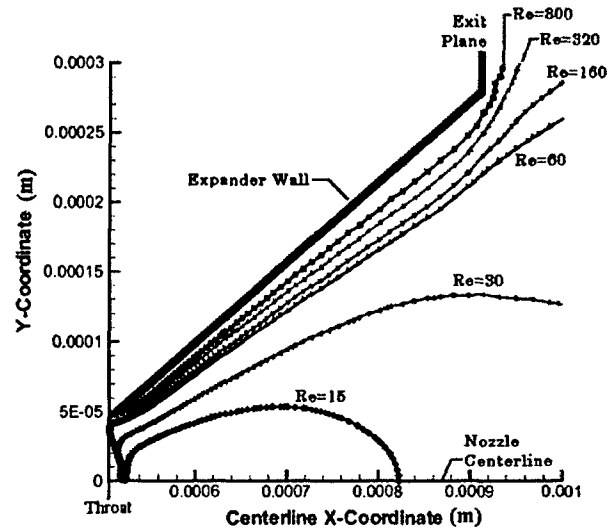


FIGURE 5. Decomposed hydrogen peroxide subsonic boundary layer thickness in the 30° half-angle nozzle expander section. The Reynolds number has been varied between $15 < Re < 800$. Note that as the Reynolds number decreases, the size of the subsonic region increases. A larger subsonic region results in decreased thruster performance and efficiency.

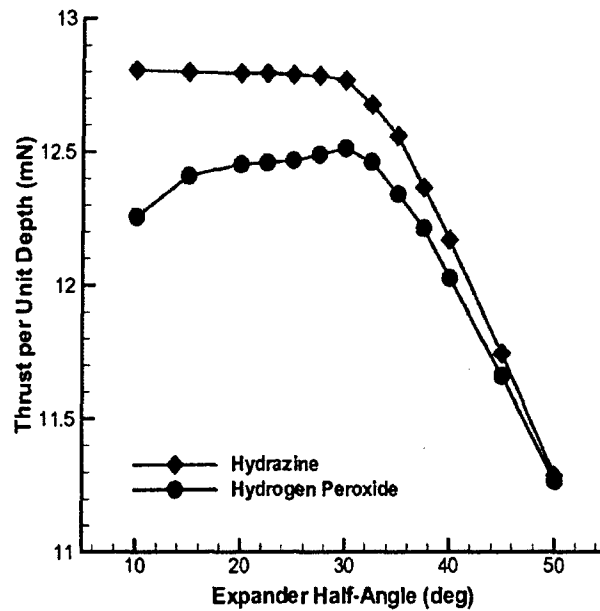


FIGURE 6. Geometry of NASA/GSFC prototype converging-diverging micro-nozzle for the monopropellant thruster. Note expander angle θ . All units are in microns. The depth of the device is varied.

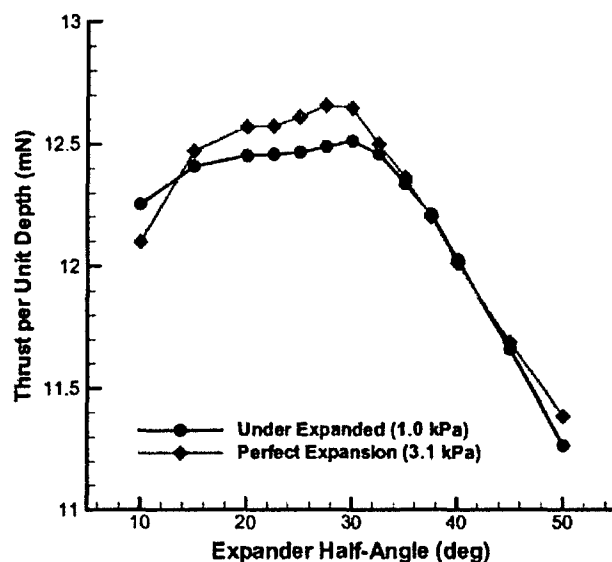


FIGURE 7. Plot of thrust in micro-Newtons per unit thruster depth as a function of expander half-angle in degrees for decomposed hydrogen peroxide. Results for both the under-expanded (1.0k Pa) and perfectly expanded (3.1 k Pa) flow regimes are shown for comparison purposes. As expected, the performance increases over the range of expander half-angles for the perfectly expanded simulations.

2.4. Effects of Heat Transfer

Given the inherently large surface area-to-volume ratio found in micro-devices, the potential for increased heat transfer from the hot nozzle gas to the surrounding solid substrate is a matter warranting investigation. There are limits, however, to the level of information that can be obtained for the NASA/GSFC prototype nozzle design. The limitations arise from three key sources: (1) the uncertainty of the surrounding substrate geometry in an actual geometry; (2) uncertainty in the baseline operating temperature of the substrate; and (3) the fact that heat transfer in a steady flow will likely be different from that of a transient flow associated with an actual thruster operational firing. In the case of the latter, mass flow profiles during an micro-valve actuation are not yet known experimentally. Here we report some preliminary results under the simplifying assumption of steady-flow and *isothermal walls of specified temperature*. The latter assumption removes the dependency on the unknown substrate parameters and replaces it by an effective heat sink whose strength can be represented by adjusting the imposed wall temperature. For the baseline flow rate and operating condition, Figs. 8-9 show a comparison of the temperature fields between a nozzle with adiabatic walls and one with walls held at a constant temperature of 200K.†. It is found that the effects of heat transfer are largely confined to the near-wall region and roughly parallels the behavior of the viscous subsonic layer. Indeed, the impact of the heat loss is to increase the thickness of the subsonic layer, consistent with expectations from based on Rayleigh flow theory. The heat transfer

† Studies were performed with a range of wall temperatures ranging from 100-300K to represent possible on-orbit nozzle thermal conditions

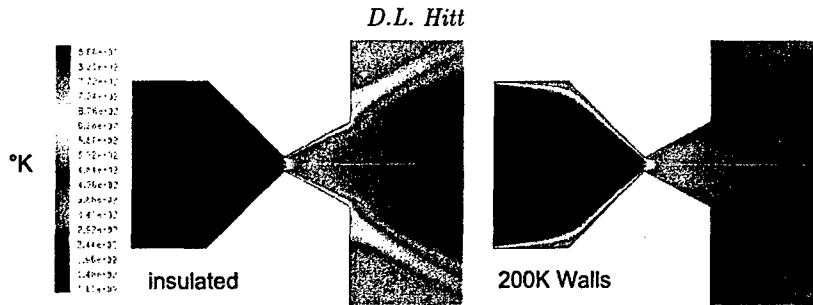


FIGURE 8. Contour plot of a steady nozzle flow under conditions of an adiabatic wall (left) and an isothermal wall at 200 K (right).

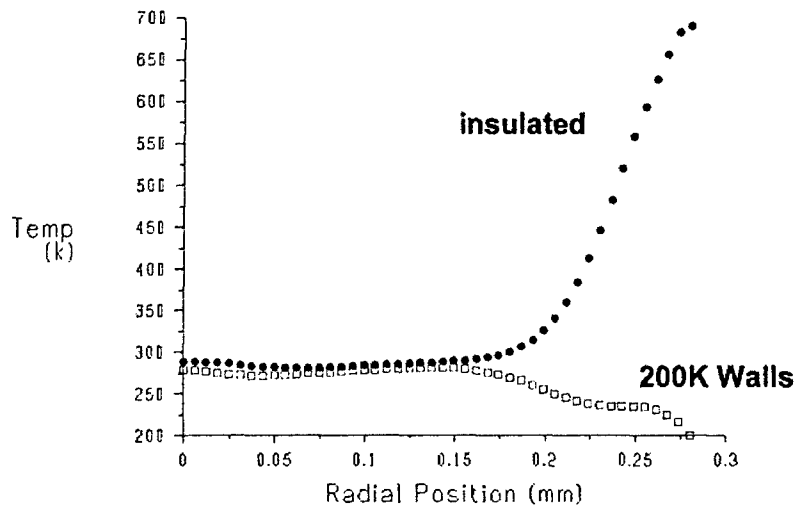


FIGURE 9. Plot of the temperature profile at the nozzle exit plane for adiabatic and isothermal (200 K) wall cases. Note that the temperature fields differ only in the vicinity of the wall.

losses ultimately manifest themselves as a loss of available energy for thrust production. Based on the simulations, we have quantified the losses as follows:

When comparing the thrust production between insulated wall and isothermal wall (at 200K) cases under baseline flow conditions, it is found that the isothermal wall cases yield thrust reductions of $\sim 2.9\%$ and $\sim 9.5\%$ for 2-D and 3-D simulations, respectively.

Here we have also alluded to 3-D results as well, as described in the section below. These results, though somewhat limited in scope owing to design unknowns, are nonetheless suggestive of the potential impact of heat transfer. It is evident that thermal analyses should be included as part of future device-specific simulations.

2.5. Exploratory 3D Simulations

The transition to a fully 3D model represents a substantial increase in computational resources and thus it was decided to pursue the 3D situation at a much lower priority than the 2D studies. To this end, by the project's completion date we have obtained

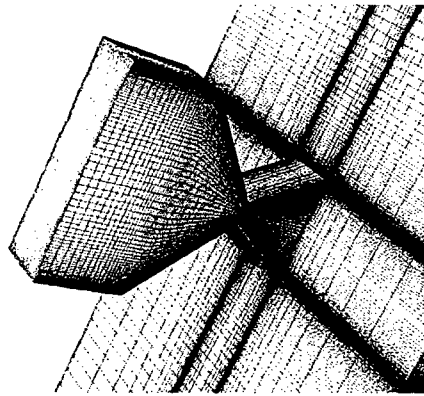


FIGURE 10. A close-up image of the computational mesh for the 3D simulations. For clarity, the surrounding ambient domain has been omitted.

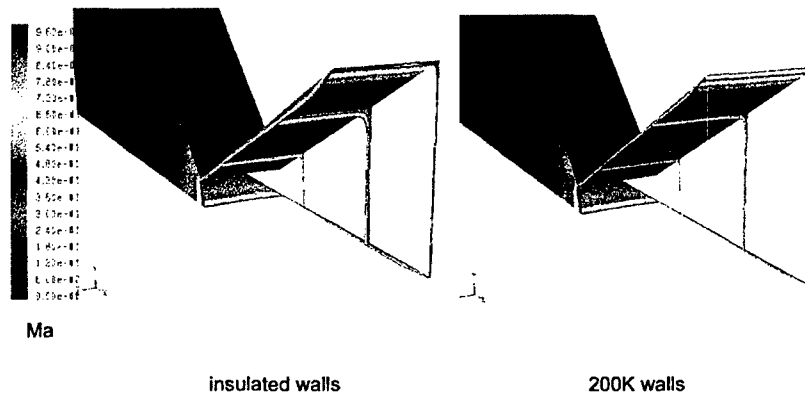


FIGURE 11. Visualization of the subsonic layers within the 3D nozzle under baseline flow conditions. Results for adiabatic walls (left) and isothermal walls (right) are shown

preliminary results for the 3D situation; nonetheless, the preliminary data is suggestive and valuable. Steady flow models with and without heat transfer have been developed to investigate the effects of a finite thruster depth ($\sim 300\mu\text{m}$ in this case). The potential impact of the 3D geometry is primarily derived from the growth of viscous layers from the top and bottom walls of the nozzle. Shown in Fig. 10 is a close-up view of the computational mesh. Illustrative results appear in Fig. 11 which provide a visualization of the viscous subsonic regions for cases of adiabatic and isothermal walls. The primary finding of these exploratory simulations is the notable reduction in thrust per unit depth compared to the 2-D planar nozzles. As with the heat transfer studies, it is clear that 3D effects should be incorporated into future design models; however, we note that the associated computational resources required will be substantial.

2.6. Transient Modeling

Much of the latest efforts were targeted at performing simulations of a more realistic transient nozzle simulation which involves the delivery of a target impulse level through

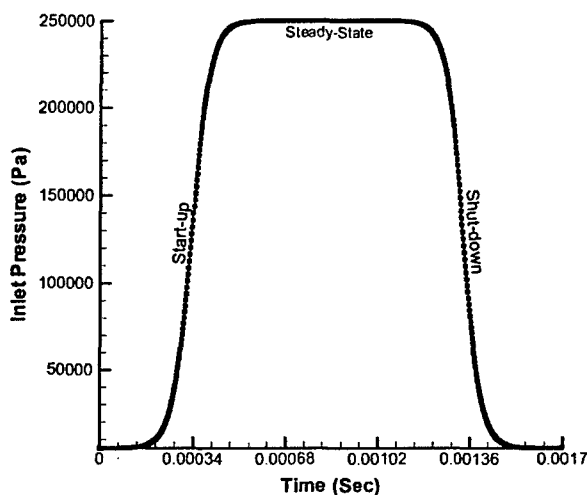


FIGURE 12. A plot of the NASA/GSFC specified actuation profile for the monopropellant delivery.

the actuation of an upstream monopropellant source. Transient simulations utilized realistic micro-valve propellant delivery data (i.e., delivery rate vs. time) from collaborating propulsion engineers at NASA/GSFC (Fig. 12). Two different monopropellants have been examined: high-concentration hydrogen peroxide (HTP) and hydrazine. For a specific monopropellant delivery profile, numerical simulations of the time-varying thrust production have been carried out for different nozzle geometries (divergence angles). Shown in Fig. 13 is a sequence of instantaneous snapshots of the nozzle plume produced at different points in the monopropellant actuation cycle. The time evolution of the viscous subsonic layer in the 30-degree nozzle is also depicted in Fig. 14; note the significant extent of this layer within the nozzle area during the course of the actuation cycle. From the simulation data, the instantaneous thrust production can be integrated to determine the total impulse delivered during the actuation cycle. The results for total impulse are plotted as a function of nozzle angle in Fig. 15. It is observed that there exists an optimum nozzle angle which maximizes performance. Owing to viscous losses, this maximum value falls short of inviscid predictions. In this case, the optimizing nozzle angle is approximately equal to that identified in steady-state simulations. However, this result will be dependent on the relative duration of the full on portion of the cycle compared to the startup/shutdown periods (i.e., the duty cycle). It may well be that for smaller duty cycles the optimum nozzle may need to be increased to accommodate the presence of larger subsonic layers (on average). The sensitivity of these results to actuation parameters remains an area of active investigation in this study

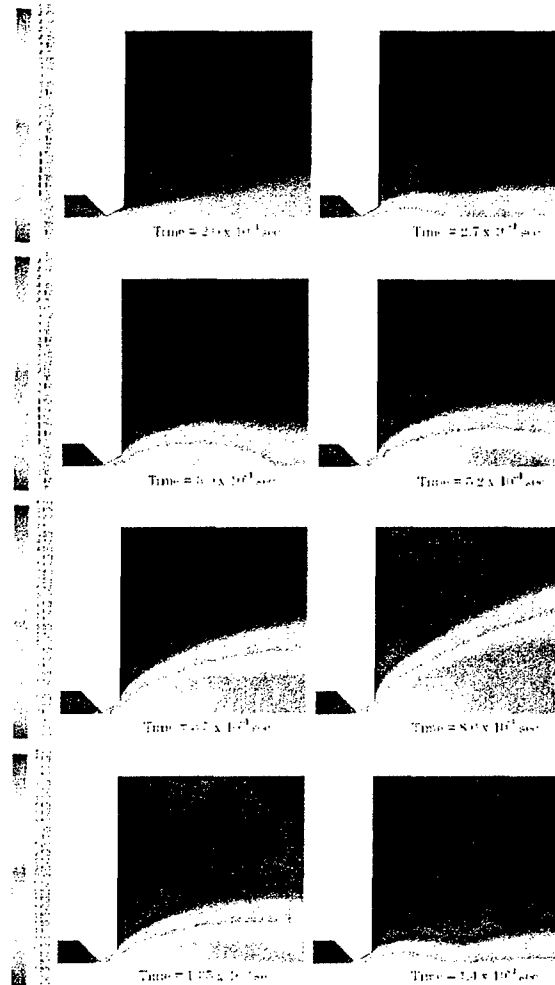


FIGURE 13. A sequence of exhaust plumes for the 30-degree expander during the transient operation of the micro-nozzle. As the pressure ratio across the nozzle increases, the plume increases in size as the flow transitions from over-expanded to under-expanded flow. An expansion fan can be seen during the steady-state portion of the cycle.

3. Modeling of Catalyzed H_2O_2 Decomposition in Microchannels

3.1. Summary of Computational Efforts

The ongoing work on this project has involved the development of semi-analytical and numerical simulations of the catalyzed chemical decomposition of hydrogen peroxide monopropellant in microchannel and/or micro-chamber geometries. As the first stage in this project, an approximate one-dimensional model for catalyzed microchannel decomposition was developed. This simplified model envisions the decomposition process as a one-dimensional reacting flow whereby the chemical decomposition serves as a non-

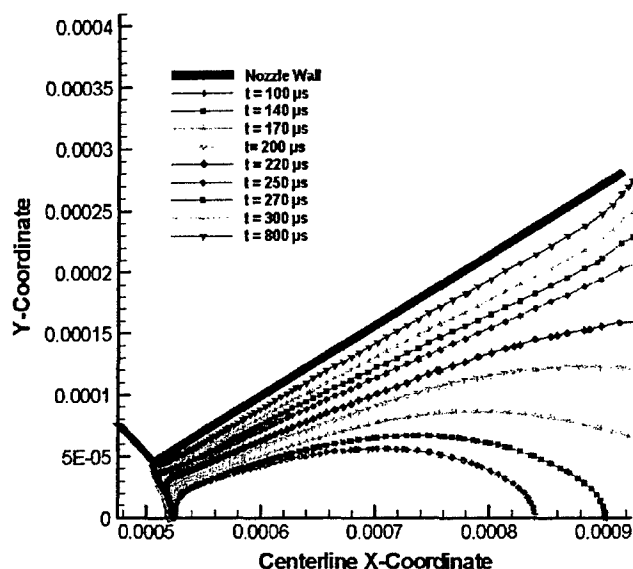


FIGURE 14. A plot of the evolution of the subsonic viscous layer within the nozzle region at different times during the actuation cycle. The lines correspond to sonic conditions (i.e., Mach 1).

linear source of heating which accelerates the rate constant. These models are reasonable approximations for 'slender' microchannel flows, and especially in situations where the catalytic material is in the form of a packed-bed (or analogous) configuration. To be precise, the term slender here refers to microchannel flows wherein the hydraulic diameter of the channel is much smaller than the characteristic length scale in the axial direction over which the complete decomposition occurs. Subsequent efforts were targeted at developing fully-computational models to perform simulations in microchannel geometries wherein the catalyst configuration is *not* that of a packed bed, but rather in the form of periodic microstructures having catalytic surfaces— which is indeed the situation for the NASA/GSFC prototype (see Fig. 16). Simulations were intended to examine the decomposition mechanism under varying flow conditions and for different catalytic materials. The ultimate goal of all modeling was to obtain an estimate of the critical (minimum) catalyst chamber length required to achieve complete decomposition. This decomposition length L was posited to depend on a number of hydrodynamic and chemical-kinetic parameters, however it is ultimately determined by the relative time scales associated with the mass flow rate and the chemical kinetics.

3.2. The Computational Models

Continuum-based computational models for the catalyzed chemical decomposition of hydrogen peroxide monopropellant were developed with specific reference to the design geometry and operating specifications of the NASA/GSFC microthruster prototype. As a strategy used to avoid the simultaneous treatment of reacting flow and phase change in the simulations, the early-stage decomposition and vaporization of the liquid monopropellant was treated separately via a simplified 1-D control volume model for the flow (see Fig. 17). Referring to Fig. 17, the vaporization of the liquid hydrogen-peroxide and

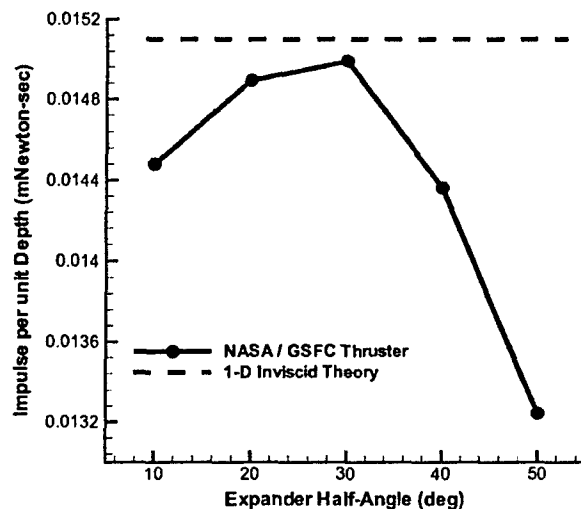


FIGURE 15. A plot of the total impulse delivered by varying nozzle angles as determined from the transient simulations. Note the existence of an optimum nozzle angle which maximizes performance; however, even this maximum value is below inviscid predictions

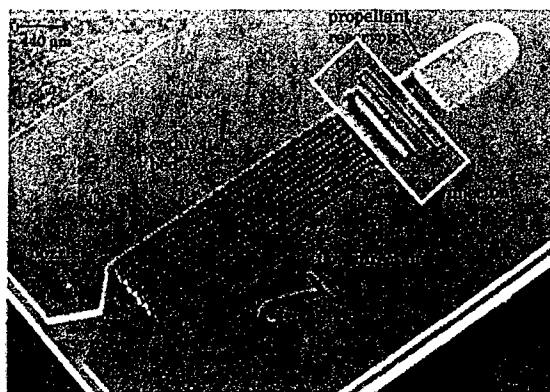


FIGURE 16. A SEM image of the prototype NASA/GSFC thruster, showing the periodic nature of the catalytic 'pillar' structures forming the catalyst chamber for the device.

water by-product occurs in Stages I-IV; thus the thermo-fluidic outlet conditions of Stage IV serve as the input to the reacting flow model. It was hypothesized – and confirmed *a posteriori* – that the length of the vaporization region was much smaller than the length required for the complete decomposition to occur. As such, any limitations of the simplified phase-change modeling had minimum impact on the ultimate determination on the critical catalyst bed length. Decomposition simulations have been performed under varying operating conditions, and have investigated the effects associated with the following parameters:

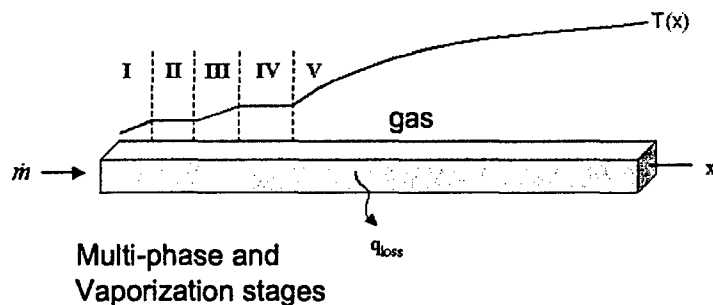


FIGURE 17. Schematic diagram depicting early stages of vaporization. Labeled as Stages I-IV, these regions reflect the initial vaporization of the liquid water/hydrogen-peroxide mixture at the inlet; Stages II and IV reflect the vaporization of the water and hydrogen peroxide, respectively. The outlet conditions of Stage IV serve as the inlet conditions for the actual numerical simulations.

- Mass flow rate
- Catalyst material
- Monopropellant inlet concentration

In non-dimensional terms, the effect of these physical parameters is best reflected by the Arrhenius chemical kinetics for the decomposition process:

$$k_* = Da \exp\left(-\frac{Ze}{T}\right) \quad (3.1)$$

where k_* is a dimensionless reaction rate, Da is the Damkohler number (a ratio of kinetic and convective time scales) and Ze is a 'Zeldovich-like number' (a non-dimensional activation energy for the catalytic material).

The approximate 1-D computational models were initially utilized to obtain basic understanding of the decomposition behavior and characteristics on the micro-scale, and also to obtain leading-order estimates of the minimum necessary decomposition chamber dimensions. The simplicity of the model greatly facilitated parametric studies without the computational overhead associated with fully-numerical simulations involving more complex domains. Later efforts targeted the development of a fully-numerical model of the chemical decomposition in a catalyst bed geometry which accurately represents that of the NASA/GSFC prototype. Shown in Fig. 18 is an image of the computational mesh used in those simulations. Note that a simplifying approximation was invoked: that the flow domain is periodic in the direction normal to the flow. Referring to the actual prototype, we see that this assumption is correct over the bulk of the catalyst bed save for the regions immediately adjacent to the two walls. The results obtained thus well characterize the decomposition dynamics within virtually all of catalytic region, and we posit that errors introduced from the near-wall regions will have minimal impact on the overall operation. The alternative of including the wall regions would render the computational domain *extremely* large and would require dramatically more computational resources; as such, this alternative was deemed impractical. Owing to tight spacing of the catalytic structures, and as a simplifying approximation, the chemical (Arrhenius) kinetics were based on a *volumetric-based* catalysis rather than directly modeling surface catalytic

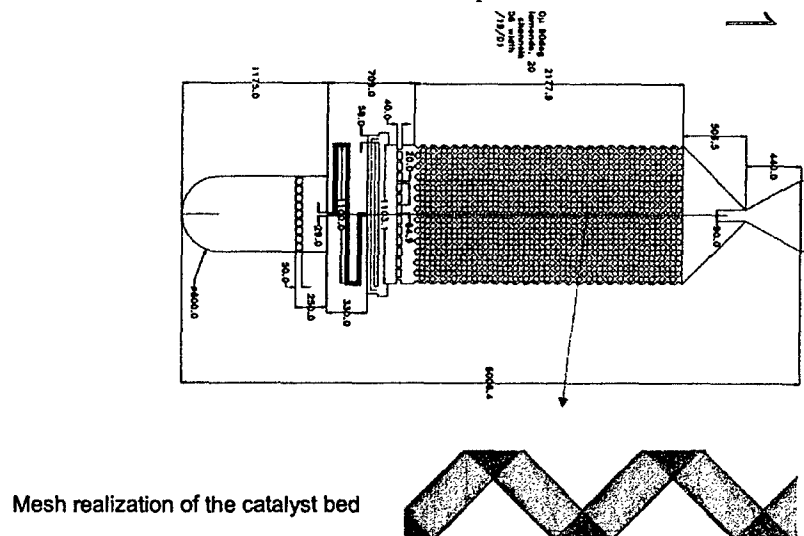


FIGURE 18. The computational mesh developed for the simulations of reacting flow in the NASA/GSFC catalyst bed geometry. The mesh is greatly simplified by the assumption of periodicity in the lateral direction.

reactions on the wall. This is an admitted limitation to the current model, and an area for future refinement.

All simulations have been performed using the FLUENT6 computational fluid dynamics software package on Linux CPU servers (Dell PowerEdge 2650, dual Xeon 2.8 GHz processors, 4 GB RAM) purchased under this grant.

3.3. Illustrative Results & Outcomes: 1-D Modeling

The intent of the one-dimensional model has been to obtain an estimate of the critical (minimum) catalyst chamber length required to achieve complete decomposition. This decomposition length, L , is shown to depend on a number of hydrodynamic, thermal and chemical-kinetic parameters. The typical decomposition behavior is well demonstrated in Fig. 19. As shown in this figure, the Arrhenius kinetics results in a thermal detonation at a point in time when the temperature has risen to a critical value due to the release of energy in the decomposition. At this detonation point the decomposition, in essence, goes to completion instantly (or very nearly so). As predicted by the form of the Arrhenius kinetics, the non-dimensional reaction rate required to reach this critical point is inversely proportional to the value of Damkohler number (Da) and the decomposition length scales accordingly (see Fig. 20). The value of Zeldovich-like number Ze establishes the threshold temperature which must be reached for thermal detonation and, owing to the Arrhenius form, the time and length required for detonation is thus *exponentially* related to Ze . The relation of decomposition length to Ze is also depicted in Fig. 20. Key findings are summarized below.

Dominance of Kinetics. Theoretical considerations clearly demonstrate the decomposition length is dominated by the chemical kinetics of the process and, to a lesser extent, the fluid mechanics. This dominance is expected to moderate somewhat in higher dimensional models but still remain essentially intact. Arrhenius kinetic assumptions for

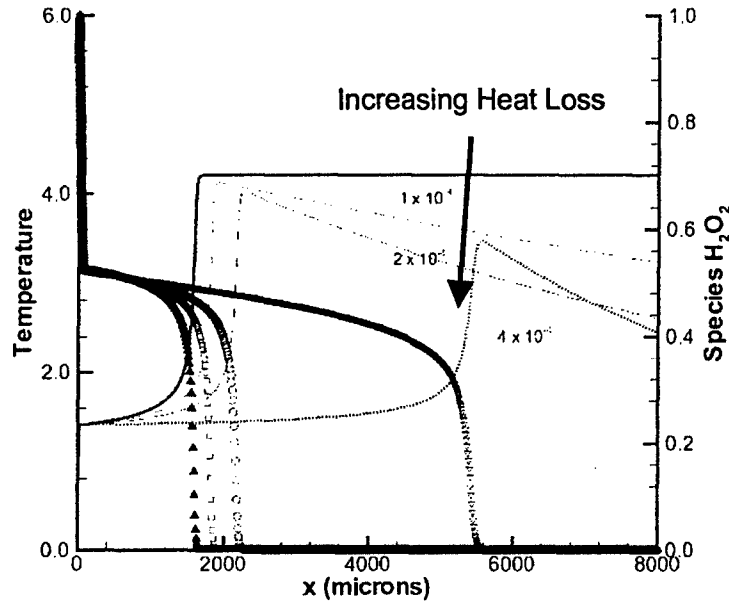


FIGURE 19. Illustrative results for a 1-D slender microchannel simulation. Shown are the temperature and species concentration as a function of downstream location; the family of profiles depict results for different levels of external heat loss into the surrounding substrate.

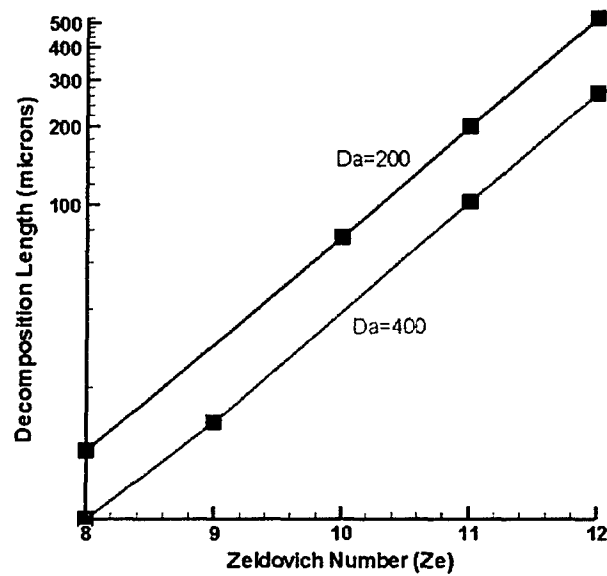


FIGURE 20. Critical decomposition lengths L for two different monopropellant mass flow rates as a function of the non-dimensional activation energy (Ze) of the catalytic material.

a general one-step, first-order monopropellant show that thermal detonation is possible for a highly efficient catalyst. It has been clearly shown that the dominant parameter is, indeed, the surface activity of the catalyst. For hydrogen peroxide, it has also been demonstrated that the traditional silver catalyst may, in fact, be replaced by much more efficient catalysts such as ruthenium-oxide (RuO_2). For example, the RuO_2 catalyst could result in surface activity 40 \times that of silver.

Critical Catalyst Bed Dimensions. Results from simulations suggest that complete decomposition in slender microchannels should be possible over lengths typically ranging from 0.6 – 2 mm which bodes well for MEMS devices. The parameters used in the simulations presented have been based upon a monopropellant thruster design capable of producing 100 μN of thrust, in conjunction with the NASA/GSFC design. As stated above, the results remain strongly dependent on catalyst properties.

Importance of Heat Transfer. External heat losses from the catalyst bed to the surrounding substrate appear to be significant on the micro-scale due to the high surface area to volume ratio and can act to delay the complete decomposition process. Shown in Fig. 19 is a family of curves subjected to different levels of heat loss as defined by a dimensionless heat transfer coefficient α . As seen in this figure, modest levels of heat loss can significantly increase minimum catalyst bed dimensions and diminish the peak temperature reached within the catalyst bed. This effect is consistent with expectations from Arrhenius kinetics since the temperature is exponentially linked with the local reaction rate. Further, the simulations have indicated that with sufficiently high heat loss the thermal detonation and even complete decomposition can be compromised.

3.4. Supporting Experiments

Supporting experiments have been conducted in collaboration with the Propulsion Branch at NASA/GSFC using a meso-scale experimental analog for the 1-D decomposition model. A glass capillary (1.2 mm ID \times 3 in. long) was been filled with a packed bed of silver micro-spheres (50 micron diameter). Using realistic mass flow rates for target micro-thrust levels, decomposition of hydrogen peroxide in this geometry has been measured indirectly by measuring temperatures at different positions along the capillary length Fig. 21 . A sample temperature data set for a start-up flow is shown in Fig. ??; referring to this figure, the cessation of data corresponded to the melting of the epoxy holding the thermocouple in place at the exit. The photograph of the exhaust plume (see Fig. 21) shows completely gaseous products exiting. Brix refractometry analysis has confirmed complete decomposition. Experimental tests for different catalyst lengths have shown that a length of ~ 1 mm for the catalyst bed produced complete decomposition, which is quite supportive of the 1-D model predictions.

3.5. Thermal Decomposition of Monopropellant

Based on the importance and efficiency of heat transfer in micro-scale geometries, we have also explored the prospect of using – exclusively – electrical heating of the monopropellant to produce accelerated decomposition via Arrhenius kinetics. This ‘thermal’ decomposition strategy was explored as an alternative to catalytic decomposition owing to the documented difficulty in creating *in situ* catalytic structures in micro-geometries and the relative ease of fabricating MEMS-based heaters. Predictions for the decomposition length as a function of volumetric heating input are shown in Fig. ?? In short, the energy requirements are rather high for nanosats owing to the high activation en-

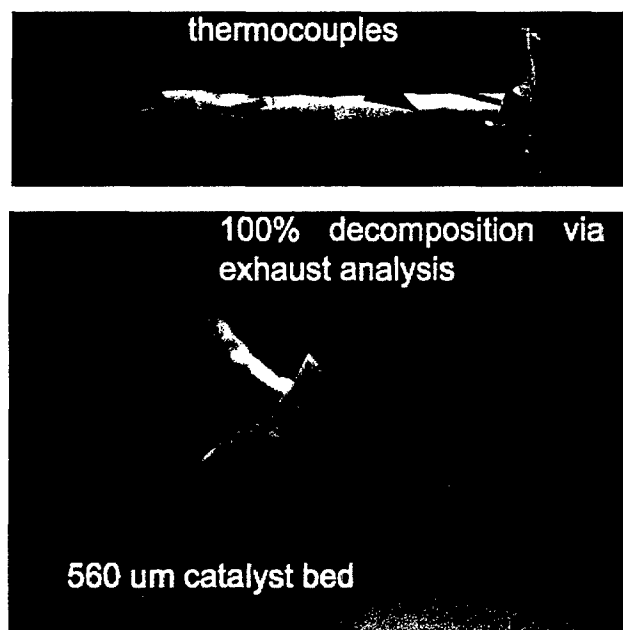


FIGURE 21. Photograph of the experiments performed to validate numerical predictions for the minimum catalyst bed length corresponding to a packed bed configuration.

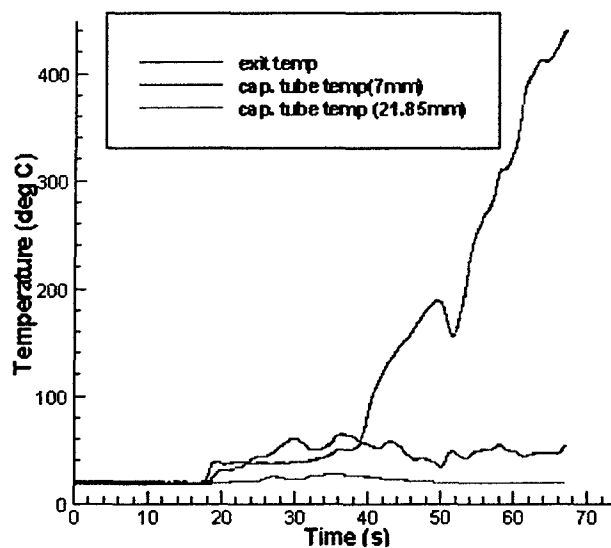


FIGURE 22. Temperature history at three points along the length of the capillary-based catalyst bed. The experimental measurements terminated when the exit temperature reached a sufficient temperature to melt the epoxy there.

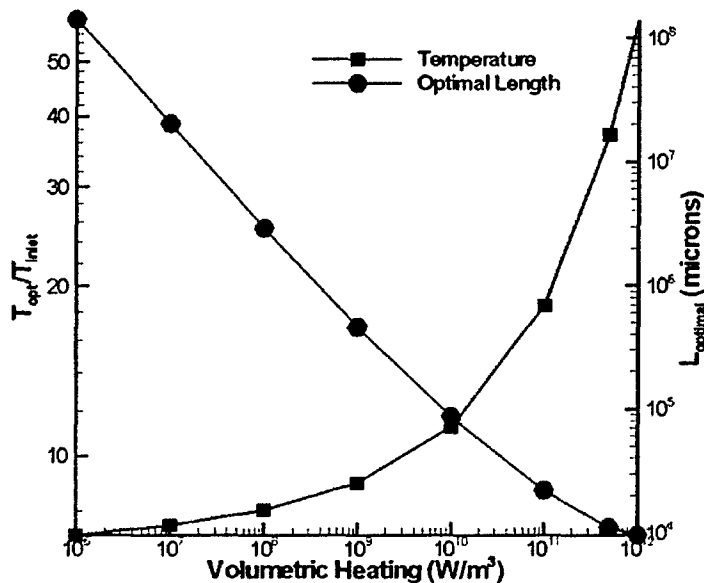


FIGURE 23. Critical decomposition lengths L based on purely thermal decomposition as a function of the volumetric heating.

ergy associated with non-catalyzed monopropellants. Thus the decomposition lengths are fairly long and, perhaps more importantly, the temperatures realized are quite high. Indeed, in most cases the theoretical temperatures would likely cause device mechanical failure. Nonetheless, the combination of catalyzed decomposition along with a modest heat input could, together, produce even smaller decomposition lengths suitable for even smaller MEMS/NEMS devices.

3.6. Illustrative Results & Outcomes: Simulations of a Micro-Catalyst Bed

Fully-computational models have been developed to perform simulations in microchannel geometries wherein the catalyst configuration is *not* that of a packed bed, but rather in the form periodic microstructures having catalytic surfaces, as with the NASA/GSFC prototype (see Fig. 18). Note that a simplifying approximation has been invoked: that the flow domain is periodic in the direction normal to the flow. Referring to the actual prototype, we see that this assumption is correct over the bulk of the catalyst bed save for the regions immediately adjacent to the two walls. The results obtained thus well characterize the decomposition dynamics within virtually all of catalytic region, and we posit that errors introduced from the near-wall regions will have minimal impact on the overall operation. The alternative of including the wall regions would render the computational domain *extremely* large and would require dramatically more computational resources; as such, this alternative was deemed impractical. Owing to tight spacing of the catalytic structures, and as a simplifying approximation, the chemical (Arrhenius) kinetics were based on a *volumetric-based* catalysis rather than directly modeling surface catalytic reactions on the wall. This is an admitted limitation to the current model, and an area for future refinement.

For the baseline design mass flow rate for the NASA/GSFC prototype, typical and

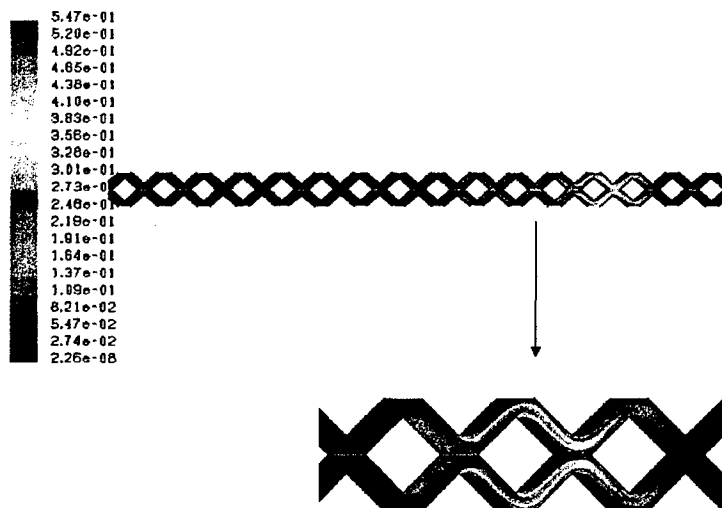


FIGURE 24. Contour plot of the hydrogen-peroxide concentration within the micro-catalyst bed. For the NASA/GSFC design flow rate, full decomposition is expected to occur within a downstream distance of approximately 1 mm.

representative decomposition results appear in Figs. 24-25. These contour plots depict the distribution of hydrogen peroxide concentration and velocity magnitude within the catalyst bed. For the NASA/GSFC design mass flow rate, full decomposition is predicted to occur within a downstream distance of approximately 1 mm, which is well within design constraints for the prototype device. However, the results have nonetheless shown to remain extremely sensitive to the Arrhenius kinetics used, and in particular the value of the activation energy associated with the particular catalytic materials.

We further note that the decomposition length predictions obtained from this catalyst bed simulation were roughly *half as small* as the predictions from the approximate 1-D models. *It is our speculation that the shorter decomposition lengths are the result of increased residence time of the fluid within the catalyst bed resulting from the flow separation around the pillar structures.*

4. Publications Resulting from AFOSR Support

The following publications related to the supported work through Spring 2006 are listed below. Copies of these manuscripts may be downloaded as PDF documents from the PI's web site at <http://www.uvm.edu/~dhitt/afosr>. This web site is password protected and requires the following username/password combination (case-sensitive):

username = afosr password = nanosat

Louisos W. and Hitt D.L., 2006, Optimal Expansion Angle for Viscous Supersonic Flow in 2-D Micro-Nozzles, AIAA J. of Spacecraft & Rockets (submitted).

Zhou X. and Hitt D.L., 2006. One-Dimensional Modeling of Catalyzed Monopropellant Decomposition in Microchannel Flows, AIAA Journal Spacecraft & Rockets (in final

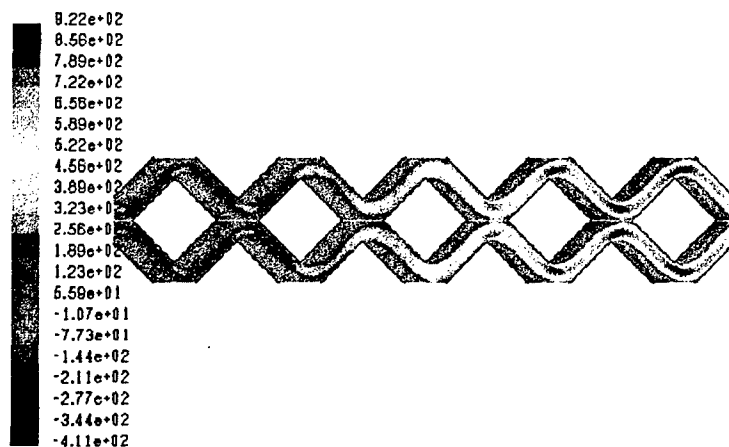


FIGURE 25. Contour plot of the gas mixture velocity magnitude within the micro-catalyst bed; note the presence of significant flow separation at the catalytic pillars.

preparation).

Zhou X. and Hitt D.L., 2006, POD Analysis of Coherent Structures in a Transient Buoyant Reacting Jet, AIAA Journal (in final preparation).

Louisos W. and Hitt D.L., 2005, Optimal Expander Geometry for Viscous, Supersonic Flows in 2-D Micro-Nozzles, AIAA Paper 2005-5032.

Zhou X. and Hitt D.L., 2005, POD Analysis of Coherent Structures in a Transient Buoyant Reacting Jet, AIAA Paper 2005-5147.

Zhou X. and Hitt D.L., 2005, Numerical Modeling of Monopropellant Decomposition in Micro-Catalyst Bed, AIAA Paper 2005-5033.

Harris T.R., Hitt D.L., and Jenkins R.G., 2005, Discrete Micro-Slug Formation for Micro-Thruster Propellant Delivery, AIAA Paper 2005-0676.

Zhou X. and Hitt, 2004, POD Analysis of Coherent Structures in a Transient Buoyant Jet, J. Turbulence, Vol. 5 (28).

Kujawa J. and Hitt D.L., 2004, Transient Shutdown Simulations of a Realistic MEMS Supersonic Nozzle, AIAA Paper 2004-3762.

Zhou X. and Hitt D.L., 2004, Modeling of Catalyzed Hydrogen Peroxide Decomposition in Slender Microchannels with Arrhenius Kinetics, AIAA Paper 2004-3763.

Zhou X. and Hitt D.L., 2003, One-Dimensional Modeling of Catalyzed H₂O₂ Decomposition in Microchannel Flows, AIAA Paper 2003-3584.

Kujawa J., Hitt D.L. and Cretu G., 2003, Numerical Simulation of Supersonic Flow in

MEMS Nozzle Geometries with Heat Loss, AIAA Paper 2003-3585.

The collection of these papers has also been sent electronically to the Program Manager at the time of this report's submission.

5. Technology Transfer Opportunities

The work that has been performed is in direct connection with actual prototype MEMS thrusters being designed and constructed in a collaboration between NASA/Goddard and the University of Vermont. Further, the work supported under this project ultimately led to a follow-on DoD EPSCoR grant from AFOSR whose intent is *to develop a working prototype thruster at the University of Vermont* using its new microfabrication facility. This prototype will ultimately be tested using the Air Force Laboratory's test facilities at Edwards Air Force Base. In short, the scientific results of this work have led – and will lead – directly into new MEMS thruster designs and prototypes.